

Seismic diagnostics of mixing beyond the convective core in intermediate mass main-sequence stars

by

B. L. Popielski¹ and W. A. Dziembowski^{1,2}

¹ Warsaw University Observatory, Al.Ujazdowskie 4, 00-478 Warsaw, Poland

² Nicolaus Copernicus Astronomical Center, ul.Bartycka 18, 00-716 Warsaw, Poland
e-mail: blapo@fuw.edu.pl, wd@astrouw.edu.pl

ABSTRACT

We study prospects for seismic sounding the layer of a partial mixing above the convective core in main-sequence stars with masses in the $1.2 - 1.9 M_{\odot}$ range. There is an initial tendency to an increase of convective core mass in such stars and this leads to ambiguities in modeling. Solar-like oscillations are expected to be excited in such objects. Frequencies of such oscillations provide diagnostics, which are sensitive to the structure of the innermost part of the star and they are known as the small separations. We construct evolutionary models of stars in this mass range assuming various scenarios for element mixing, which includes formation of element abundance jumps, as well as semiconvective and overshooting layers. We find that the three point small separations employing frequencies of radial and dipole modes provide the best probe of the element distribution above the convective core. With expected accuracy of frequency measurement from the space experiments, a discrimination between various scenarios should be possible.

Key words: *stars: variable, stars: oscillations, stars: solar-type, stars: convection*

1. Introduction

The extent of mixing beyond the convective core has been debated for several decades and the issue remains unsettled. For stars with masses above $1.9 M_{\odot}$ in the main-sequence evolutionary phase the convective core shrinks in mass and the issue concerns the extent of the overshooting beyond the boundary determined by Schwarzschild criterion (1906), which in this case is identical to Ledoux criterion (1947). At lower masses there is a tendency for the convective core expansion. Outside of the expanding core, in the environment more abundant in hydrogen, the radiative temperature gradient must be higher than below. Consequently, according to Schwarzschild criterion, such layer must be unstable. It is known (e.g. Kato, 1966) that in the latter case the instability takes form of growing oscillatory mode. The nonlinear development of the motion in the layers with preexistent chemical inhomogeneities is particularly difficult to study.

This problem has been first encountered by Schwarzschild and Härm (1958) at very high stellar masses, above $30 M_{\odot}$. In the case of these very massive stars the growth of the core was caused by the temperature increase in time, hence lowering $\beta = p_{gas}/p$, hence lowering adiabatic gradient, ∇_{ad} . To overcome the problem these authors introduced the concept of semiconvective zone outside the convective core, where hydrogen abundance rises steadily in such a way that convective neutrality is preserved. They presumed that in this layer there is a slow convection which carries negligible amount of energy, but sufficient for the required partial mixing.

In the stars with masses lower than $1.9 M_{\odot}$, the tendency for core expansion is caused by an increase of relative contribution of CNO cycle to energy production, which results in an increase of radiative gradient. This was first observed by Crowe and Mitalas (1982), who followed Schwarzschild and Härm (1958) recipe. A physical support for the semiconvective model came from Stevenson (1979), who argued that occasional wave breaking enforces the neutral stability according to Schwarzschild criterion. This argument was subsequently questioned by Spruit (1992), who inspired by simple terrestrial experiment, argued that a thin layer with very steep rise of hydrogen abundance gives rise to an entropy barrier force preventing element mixing. Above this layer there would be another convective zone. Numerical simulations of Biello (2001) provided certain support for Stevenson's picture. However, we should stress that in his simulations the adopted Prandtl number was substantially higher than in stars. These two scenarios do not exhaust all the possibilities. There is no reason to assume that overshooting stops entirely as soon as the tendency to core expansion appears. Overshooting may erase the hydrogen abundance jump above the expanding core. For this reason in addition we will also consider scenarios with adjustable overshooting distance.

We believe that the best prospect for distinguishing between various scenarios may come from analysis of solar-type oscillation frequencies. In the mass range $0.9 - 2 M_{\odot}$ we expect excitation of high order acoustic oscillations (p-modes) by the same mechanism that excites solar oscillation (Houdek *et al.* 1999). In fact the prediction is that the intrinsic oscillation amplitudes in these more massive stars would be higher than those in the Sun.

We will show in this work that with the accuracy of frequency measurements expected from dedicated space missions like COROT (Baglin *et al.* 2002), MOST (Walker *et al.* 1998) or EDDINGTON (Roxburgh and Favata 2003) we will be able to distinguish various models of element mixing in deep stellar interior.

In Section 2. we describe three scenarios for mixing above the expanding core. There we also give a short overview of our modeling procedures. In Section 3. we introduce two types of small separations. The small separations are further used to examine the effect of mixing in a grid of models across the domain of solar-like stars (Section 4.1.). The possibility of distinguishing chemical profiles through small separations is discussed in the next section (Section 4.2.). We summarize our

work in Section 5.

2. Alternative models of element mixing above the expanding core

In our work we consider three mixing scenarios in evolutionary models. Going from minimum to maximum extent of element mixing, we examine:

1. the layered model (LY),
2. the semiconvective model (SC),
3. the overshooting model (OV).

The LY model is based on Spruit (1992) scenario. We approximate the two steep hydrogen abundance rises by two composition jumps at the edges of the convective regions, as seen in Figure 1. The discontinuities of density are explicitly taken into account in calculation of our stellar models and their oscillation properties. The SC model has both density and temperature gradient continuous. However, the second derivatives of density and temperature are discontinuous at both edges of the semiconvective zone. In the OV model, the extent of the overshooting above the convective core is determined by the product $\alpha_{ov}H_p$, where α_{ov} is an adjustable dimensionless parameter and H_p is the pressure distance scale calculated at the edge of the core. Here we adopt smooth abundance profile, leading to continuous density and its derivative. The profile of hydrogen abundance in the overshooting zone, $[r_0, r_1 = r_0 + \alpha_{ov}H_p]$, is given by $X(r) = X(r_0) + y(z)$, where

$$y(z) = z^s [(X' - s\Delta X)z - X' + (s+1)\Delta X], \quad (1)$$

$$z = \frac{r - r_0}{r_1 - r_0}, \quad \Delta X = X(r_1) - X(r_0), \quad X' = (r_1 - r_0) \left. \frac{dX}{dr} \right|_{r_1} \quad (2)$$

and $s > 1$ is adjustable shape parameter. The standard overshooting model is represented by $s \rightarrow \infty$. In Figure 1 we show hydrogen abundance profile obtained with different scenarios.

The influence of rotation on mixing is not necessarily negligible, however its detailed discussion is beyond the scope of our paper.

In our code, which is an updated version of Paczyński's stellar evolution code (1970)¹, the chemical evolution is computed in an implicit way. This requires additional routine to iterate element abundances but is quite important to accurately follow the boundaries of convective and semiconvective zones. The chemical iteration scheme is not new. It was used e.g. by Crowe and Mitalas (1982), VandenBerg (1983) and Shaller *et al.* (1992).

The code includes:

¹Most of updates were made by M.Kozłowski and R.Sienkiewicz.

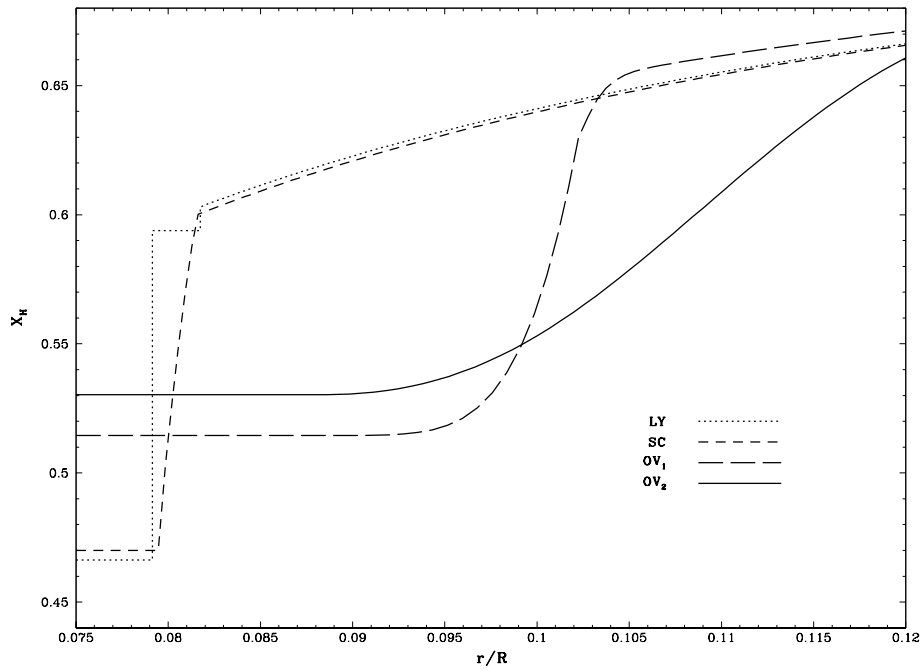


Figure 1: Hydrogen abundance profile in the layer above the convective zone for a set of slightly evolved $1.5 M_{\odot}$ models. Four curves refer to four mixing scenarios: layered, LY, semiconvective, SC, and two types of overshooting, OV_1 and OV_2 , where $\alpha_{ov} = 0.2$ and 0.5 respectively. The four models have the same radius of $1.68 R_{\odot}$.

- the radiative opacities from OPAL project (Iglesias and Rogers, 1996), the molecular opacities from Alexander and Ferguson (1994),
- the equation of state EOS2001 from OPAL project (Rogers, 2001),
- the heavy element distribution from Grevesse and Noels (1993).

The oscillation properties of models were calculated using a standard linear pulsation code (Dziembowski, 1977), where the discontinuity was explicitly taken into account.

3. Small separations

The layers that we want to probe are located very close to the center. Low degree high order p-modes reach down-there, however the question is whether there is enough sensitivity to changes in this region to expect measurable effects. The frequency combinations known to be particularly sensitive to stellar interior are familiar small separations, see Christensen-Dalsgaard (1988), defined as

$$d_{\ell,\ell+2}(n) = \nu_{n,\ell} - \nu_{n-1,\ell+2}, \quad (3)$$

for $\ell = 0$ and 1. Instead of d_{13} it is better to use the three point separations, d_{01} , as Roxburgh (1993) proposes,

$$d_{01}(n) = \frac{\nu_{n,1} - 2\nu_{n+1,0} + \nu_{n+1,1}}{2}. \quad (4)$$

because at $\ell = 3$ we expect a considerable amplitude reduction.

First analytical expressions for small separations were derived by Tassoul (1980) from a simple dispersion relation. However, her approximation is not satisfactory at quantitative level, as pointed by Roxburgh and Vorontsov (1994), who derived improved expressions. The price is that their complicated formula is not revealing. Therefore in our work we rely solely on numerical calculations of eigenfrequencies.

4. Discriminating between different mixing scenarios with small separations

4.1. Frequency dependence of small separations

The frequency dependence of small separations is not monotonic. Figure 2 shows typical examples of d_{02} and d_{01} . Regardless of the mixing scenario, there is an overall similarity of the ν -dependence shapes. There is always a minimum of d_{02} at $\nu = 750\mu\text{Hz}$ and a corresponding maximum of d_{01} at the same frequency. The d_{02} maximum at $\nu = 1500\mu\text{Hz}$ corresponds to minimum of d_{01} .

The upper limit of considered frequencies is set by ν_{cutoff} , which may be regarded as the highest frequency of the modes we may ever expect to be seen in

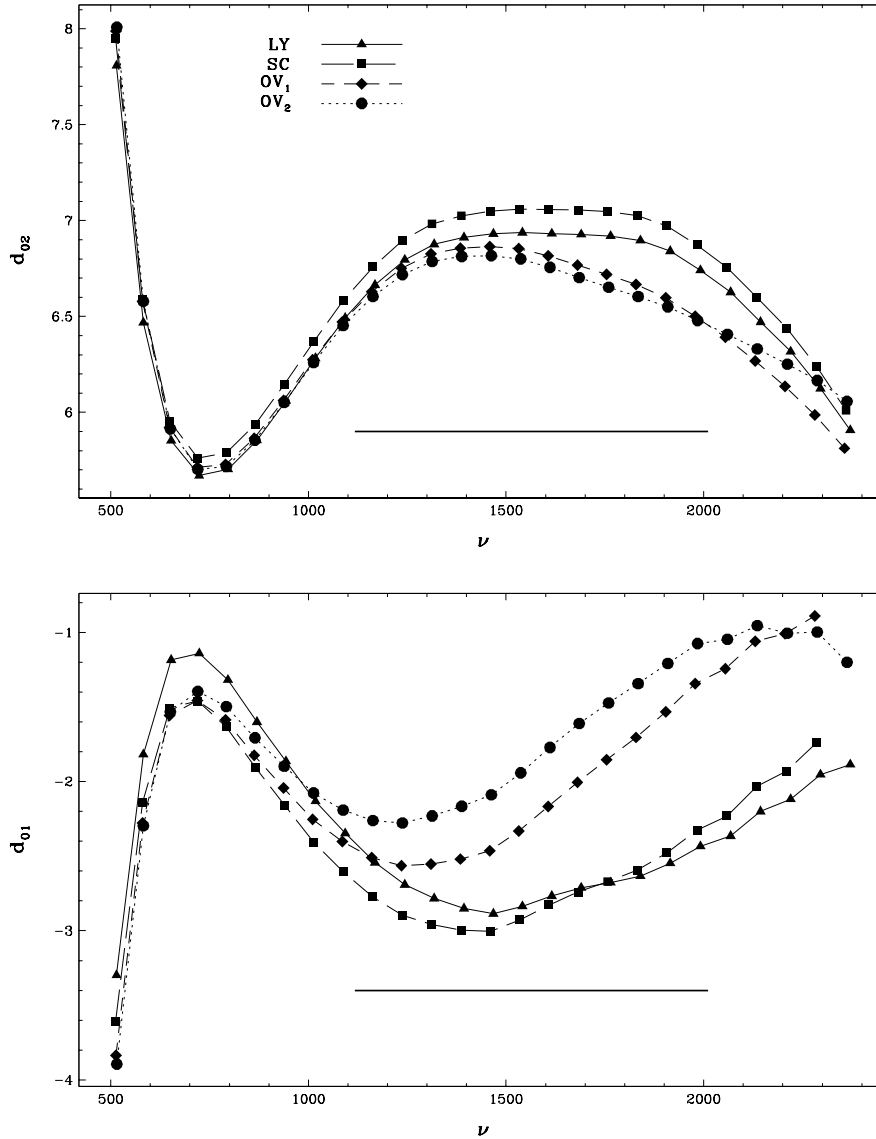


Figure 2: Small separations for the four models from Figure 1, layered, LY, semi-convective, SC, and two extents of overshooting, OV_1 and OV_2 . The mean large frequency separations for the models are equal, $\bar{D}_0 = 74.5\mu\text{Hz}$. Thick horizontal line encompasses the n-range, defined in the text. We see that there is more sensitivity to mixing scenarios in d_{01} (lower panel).

object	frequency range [μHz]	\overline{D}_0	n	references
α Cen A	1675 \div 3055	106.2	16 \div 29	Bedding <i>et al.</i> (2004)
η Boo	600 \div 1100	40.5	15 \div 27	Kjeldsen <i>et al.</i> (2003)
Procyon A	300 \div 1400	53.6	6 \div 26	Martić <i>et al.</i> (2004)
Sun	2400 \div 3700	135.5	8 \div 33	Gabriel <i>et al.</i> (1997)

Table 1: Ranges of frequency data for solar-like stars. Corresponding radial orders, n , are derived from the mean large frequency separations, \overline{D}_0 . The solar data refers to low spherical degree modes whose frequencies are accurately determined.

distant stars. Although the peaks in the solar oscillation spectrum are seen above this frequency, they are low and broad. The lower limit is set arbitrarily by an approximate validity of asymptotics. However, the frequency that we may expect to measure in the near future belongs to a significantly narrower range. The horizontal line encompasses the range of mode orders, $n = 15 \div 27$, we are most likely to detect. In determining this range we were guided by currently available oscillation spectra for distant stars and by the frequency range of low degree solar oscillation modes usable in helioseismic sounding. The summary of the observational information relevant for determining this range is given in Table 1.

4.2. The survey

In order to see how the different mixing scenarios influence the small separation, we consider 3D family of models in the mass range from 1.2 to 1.7 M_\odot , which encompasses most of the stars with expanding convective cores.² We assume the mixing length parameter $\alpha = 1.5$ and standard population I chemical composition ($X=0.7$, $Z=0.02$). The models are characterized by mass, the mean large frequency separation and the mixing scenario. The grid of models considered in various mixing scenarios is given in Table 2. The models cover the early phase of the main sequence evolution which in the case of the LY and SC scenarios is characterized by the convective core expansion. Evolutionary tracks for selected masses and two mixing scenarios (SC, OV_1) are shown in Figure 3. There, the positions of the selected models are shown with symbols. The tracks calculated with LY scenario are nearly identical to the tracks calculated with SC scenario. The departure of the OV_2 tracks from SC tracks is similar to that of OV_1 tracks, but larger. The parameters characterizing the evolutionary state of the core in selected models are given in Table 3.

The $d(\nu)$ dependence in models of our survey are plotted in Figures 4 – 8. We may see that within the n -range there is a large variety in shapes of the ν -dependence. We see both monotonic increase and decrease, as well as occurrence of extrema. There is a striking difference in the behavior of d_{01} and d_{02} . The former exhibits significantly larger sensitivity for the adopted mixing scenario. Therefore

²We exclude the stars with higher masses, for which the expansion of convective core is negligible.

	Mass [M_{\odot}]			
\overline{D}_0 [μHz]	1.2	1.3	1.5	1.7
93.8	M2a			
91.0	M2b	M3b		
81.6	M2c	M3c	M5c	
74.5		M3d	M5d	M7d
53.6		M3e	M5e	M7e
42.3				M7f

Table 2: Grid and nomenclature of models used in the survey. The names of the models contain decimal digit of the mass and a letter, which stands for the mean large frequency separation.

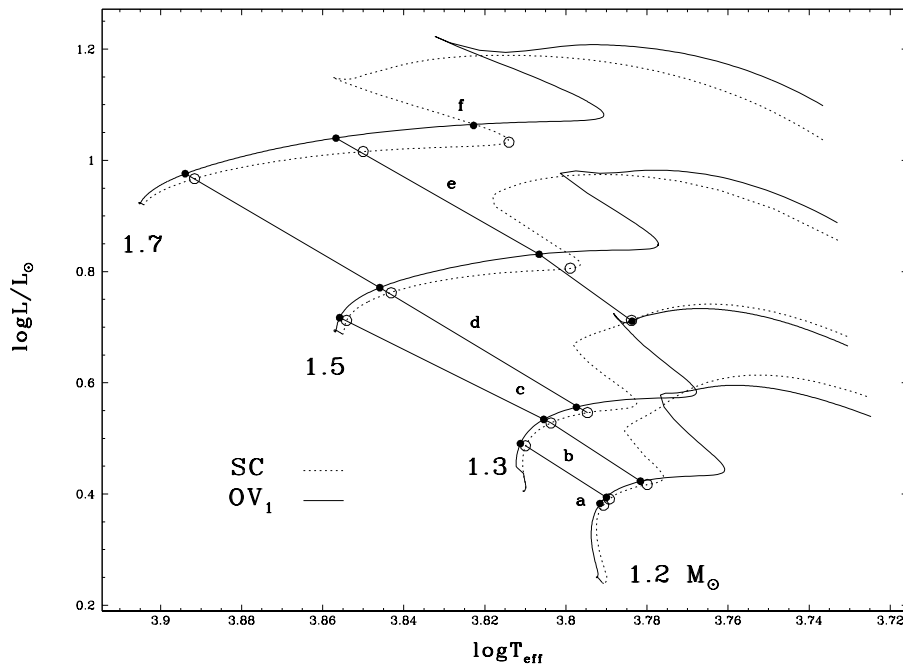


Figure 3: Evolutionary tracks calculated with the two mixing scenarios, SC and OV_1 . The models selected for the survey of small separations are marked with open and full circles for SC and OV_1 , respectively. The models of the same \overline{D}_0 are connected. The connecting lines are accompanied by a letter, which indicates the value of mean large frequency separation, \overline{D}_0 .

	LY				SC				OV ₁				OV ₂			
	X_c	x_{cc}	m_{cc}		X_c	x_{cc}	m_{cc}		X_c	x_{cc}	m_{cc}		X_c	x_{cc}	m_{cc}	
M2a	0.291	0.046	0.021	exp	0.304	0.048	0.022	exp	0.425	0.088	0.104	cont	0.509	0.125	0.222	cont
M2b	0.248	0.048	0.024	exp	0.276	0.051	0.029	exp	0.390	0.085	0.101	cont	0.488	0.122	0.220	cont
M2c	0.083	0.047	0.036	cont	0.143	0.054	0.047	cont	0.266	0.077	0.100	cont	0.406	0.111	0.216	cont
M3b	0.474	0.085	0.034	exp	0.479	0.086	0.036	exp	0.544	0.098	0.117	cont	0.587	0.132	0.248	cont
M3c	0.323	0.095	0.053	exp	0.335	0.097	0.055	exp	0.421	0.088	0.116	cont	0.504	0.120	0.230	cont
M3d	0.206	0.096	0.059	cont	0.223	0.099	0.052	cont	0.324	0.081	0.115	cont	0.440	0.111	0.222	cont
M3e	0.000	0.000	0.000	–	0.000	0.000	0.000	–	0.000	0.000	0.000	–	0.185	0.082	0.197	cont
M5c	0.565	0.083	0.079	exp	0.565	0.084	0.080	exp	0.592	0.108	0.154	cont	0.616	0.137	0.264	cont
M5d	0.466	0.079	0.085	exp	0.467	0.079	0.087	exp	0.510	0.100	0.151	cont	0.530	0.108	0.183	cont
M5e	0.065	0.050	0.064	cont	0.091	0.052	0.070	cont	0.237	0.074	0.137	cont	0.367	0.097	0.235	cont
M7d	0.539	0.095	0.111	exp	0.546	0.096	0.112	exp	0.572	0.116	0.180	cont	0.592	0.140	0.278	cont
M7e	0.260	0.146	0.095	cont	0.270	0.069	0.096	cont	0.352	0.088	0.165	cont	0.417	0.107	0.249	cont
M7f	0.035	0.114	0.065	cont	0.054	0.048	0.069	cont	0.207	0.082	0.158	cont	0.316	0.089	0.238	cont

Table 3: Characteristics of the convective core for the models of our survey. X_c denotes central hydrogen abundance, x_{cc} – fractional radius of the core, m_{cc} - fractional mass. "exp" and "cont" stands respectively for the core expanding and contracting (in mass). For the OV models, for which the chemical profile is smooth, we use the effective size of the core.

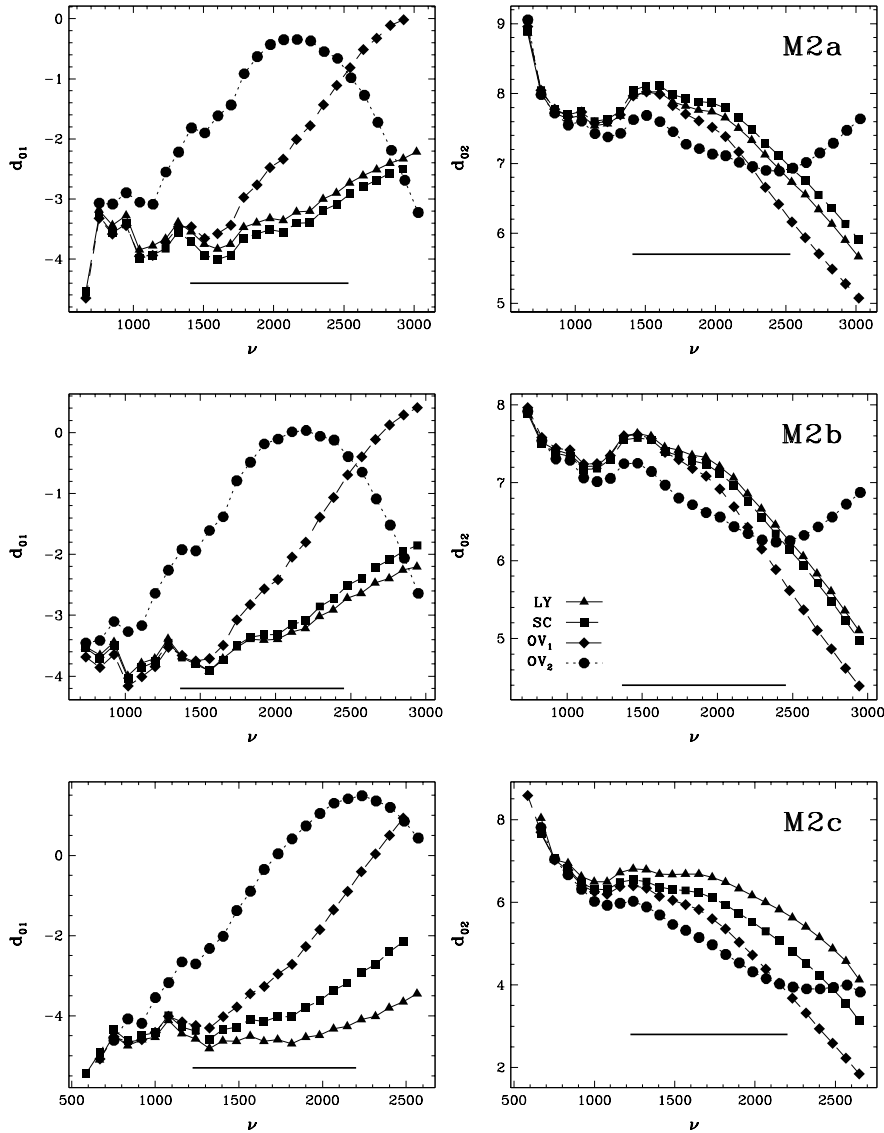


Figure 4: Small separations for $1.2 M_{\odot}$ models of the survey. The rows correspond to models and the columns to different small separations, d_{01} and d_{02} . Horizontal line on each panel spans the radial order range, $n = 15 \div 27$ – see Section 4.1.

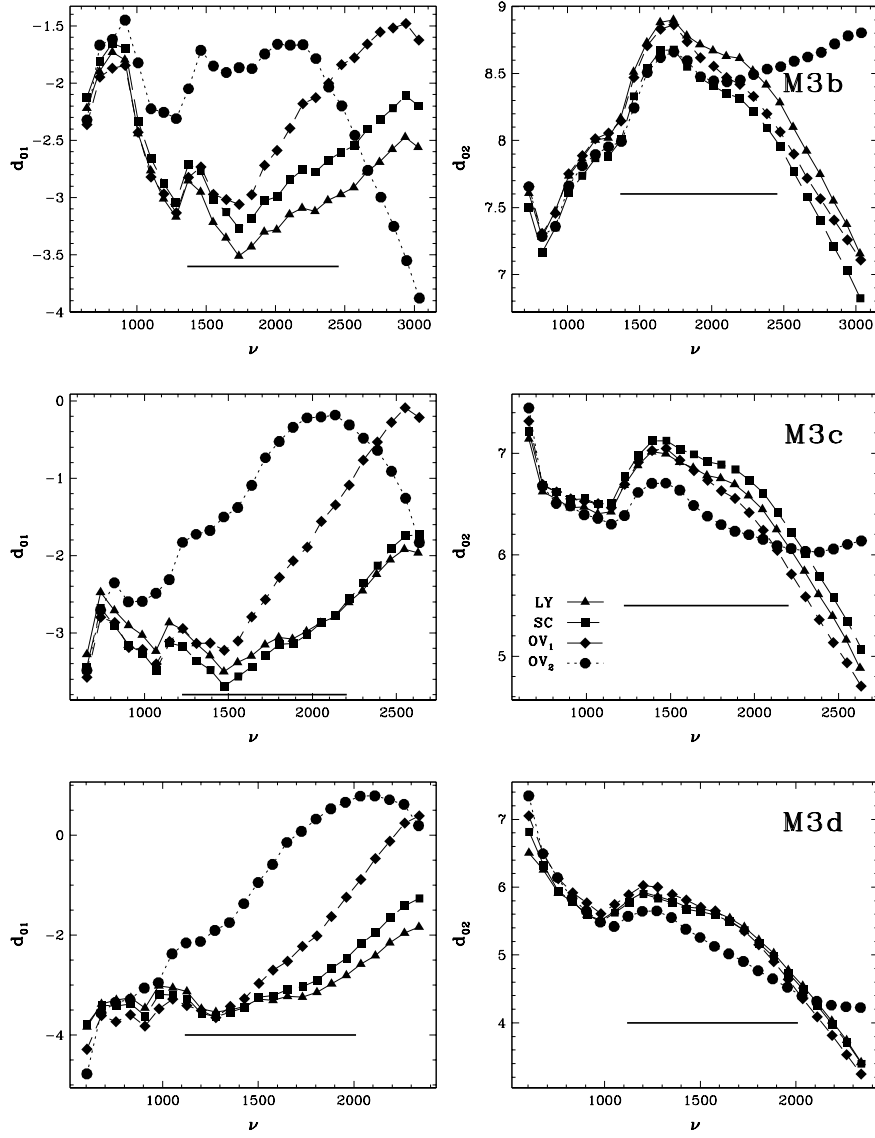


Figure 5: Small separations for $1.3 M_{\odot}$, as in Figure 4.

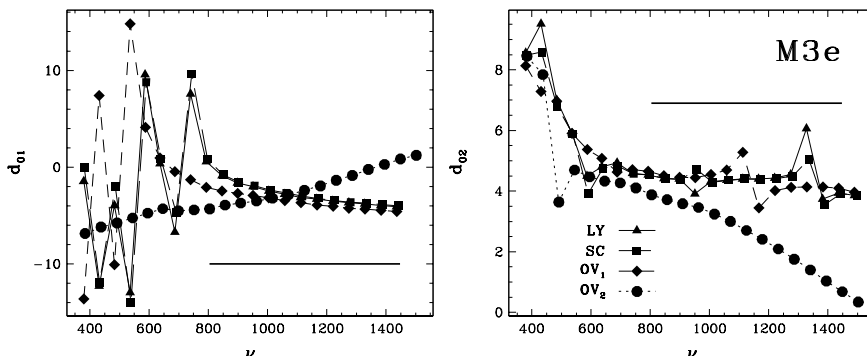


Figure 6: Small separations for an evolved model of $1.3 M_{\odot}$, as in Figure 4.

we concentrate our attention on the behavior of the d_{01} separation.

We will characterize d_{01} in various models by two parameters, the mean value over the considered range of mode orders, \bar{d} , and the normalized mean slope,

$$d_S = \bar{D}_0 \frac{\partial d_{01}}{\partial \nu},$$

where the derivative is determined by the linear fit of $d_{01}(\nu)$. Now, each model is represented by two quantities \bar{d} and d_S , which may be measured. These are plotted in Figure 9 for all the models except of M3e, which represents the post main-sequence phase. The parameters α , X and Z influence the $\bar{d} - d_S$ diagram, but within the reasonable ranges the effect is not large. The most interesting feature is that models are grouped in the diagram according to the mixing scenario. This means that even without precise knowledge of star parameters there is a chance of discriminating between various scenarios. We see that the most negative values of \bar{d} correspond to the LY scenario, that is least mixed models. Moving upward we go in the direction of more extensive mixing. The value of d_S reflects primarily the evolutionary status of the star.

Admittedly, the most difficult may be discriminating between the LY and SC scenarios. We may see in Figure 9 that the largest differences in \bar{d} between the models calculated with the LY and SC scenarios at fixed mass and \bar{D}_0 do not exceed $1 \mu\text{Hz}$. There are various assessments of the accuracy of frequency measurements in planned space missions. The optimistic error estimate of individual frequency data is $0.1 \mu\text{Hz}$ (Baglin *et al.* 2002). Thus there is a prospect for disentangling the two scenarios but the objects must be carefully chosen. The models leading to the largest differences in \bar{d} are M2c and M5e, which correspond to the phase of vanishing convective core. All models with intermediate masses between 1.2 and $1.7 M_{\odot}$ in the similar evolutionary phase show similar differences in \bar{d} . None of the models with $M = 1.3 M_{\odot}$ shown in Figure 9 reached this phase yet. Thus the most suitable objects are stars near the end of the main-sequence phase.

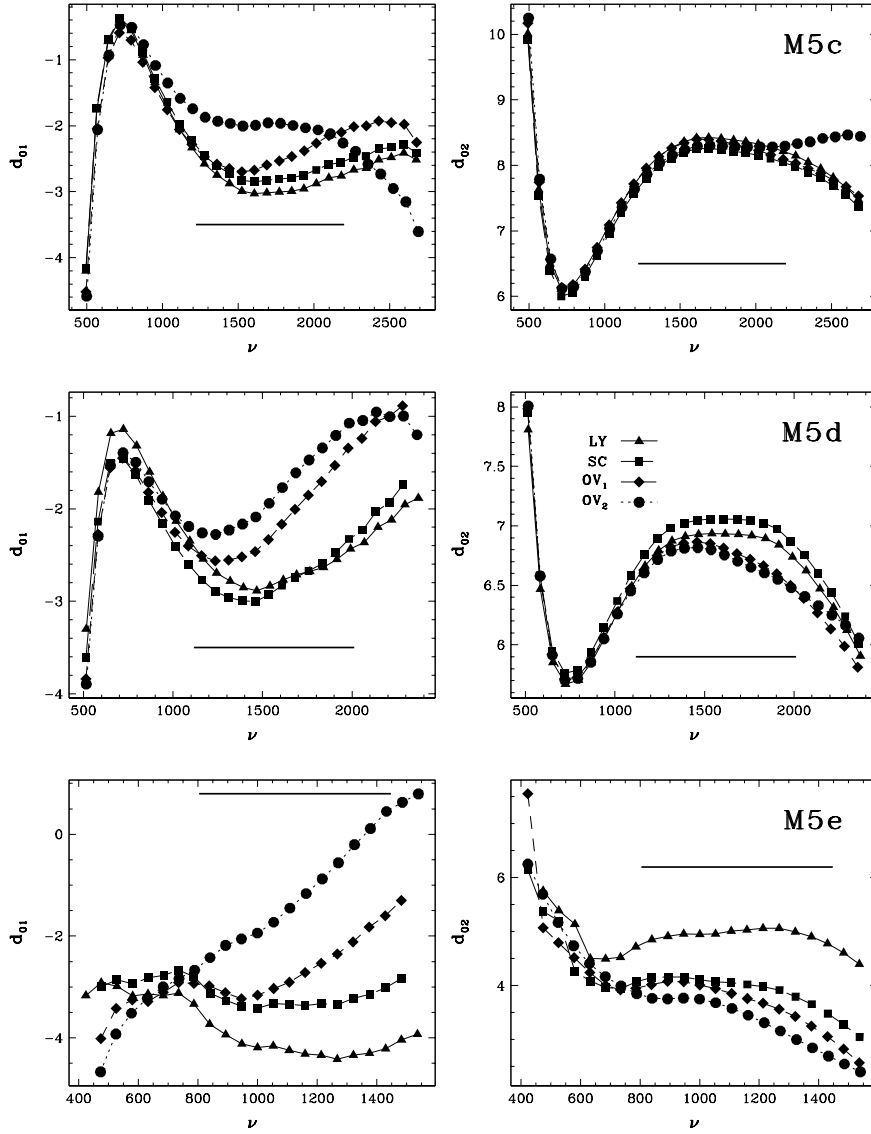


Figure 7: Small separations for $1.5 M_{\odot}$, as in Figure 4.

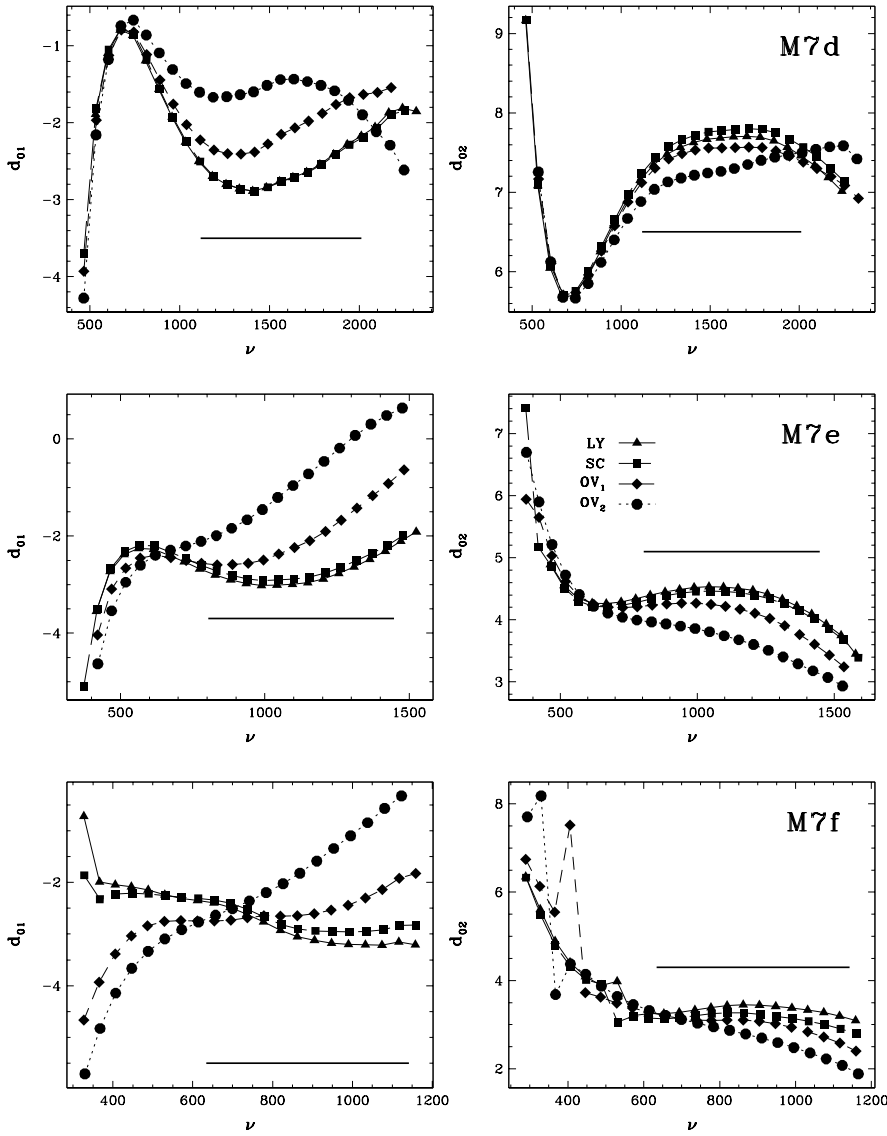


Figure 8: Small separations for $1.7 M_{\odot}$, as in Figure 4.

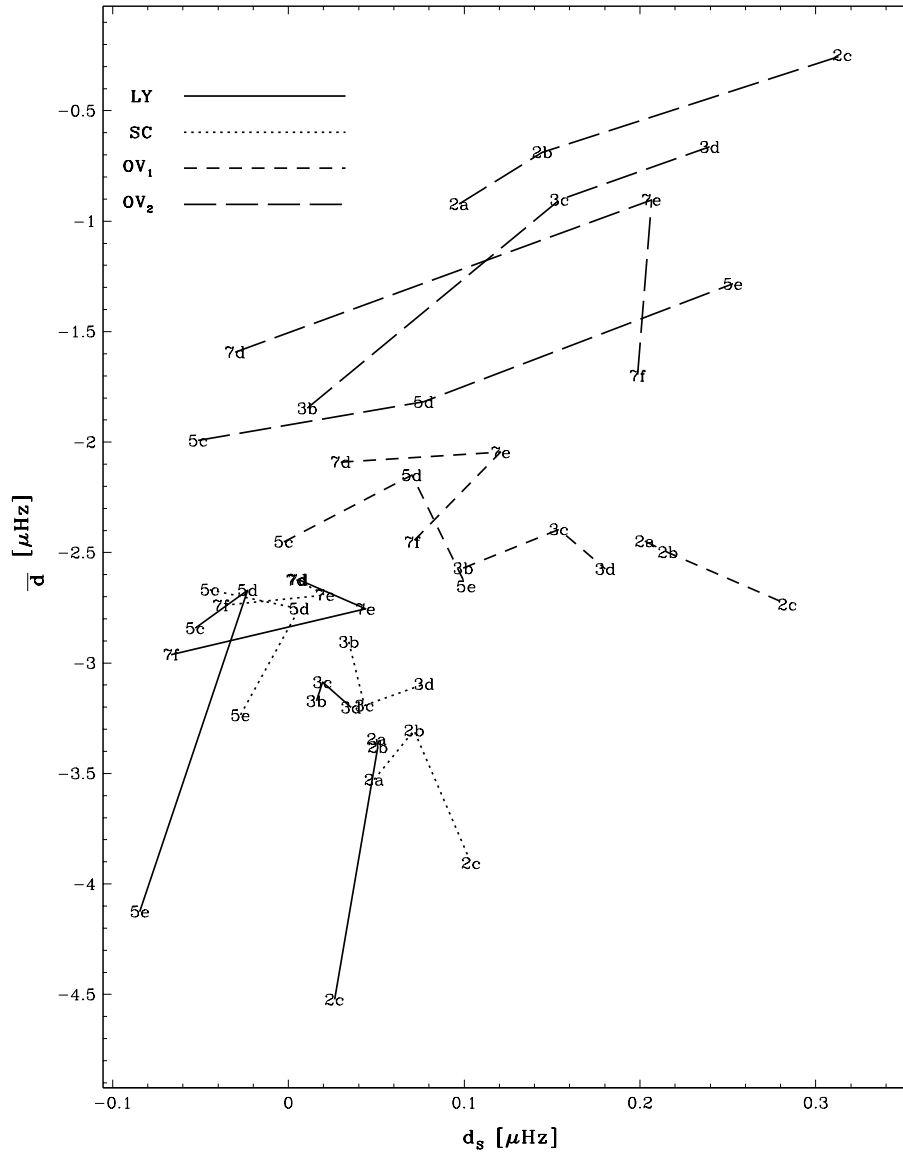


Figure 9: Two parameters characterizing d_{01} in models with various mixing scenarios.

Models calculated assuming extensive overshooting lay well above those calculated with either LY or SC scenario. Thus there should be no difficulty in discriminating between the extensive and weak mixing scenarios.

The diagnostic utility of the $\bar{d} - d_S$ diagram is not restricted to main-sequence stars. The signature of the mixing processes above an expanding core is present until the hydrogen burning shell wipes it out. For example, the discontinuity arising in the LY scenario persists in the $1.3 M_\odot$ model for 0.6 Gyr past the main-sequence phase, which is about 1/5 of the main-sequence lifetime. Once the shell source enters the part of the profile that is unreachable for mixing processes connected to the convective core, all the memory of different mixing scenarios is erased. Figure 10 shows the evolution of $1.3 M_\odot$ models in the $\bar{d} - d_S$ diagram through the main-sequence and early post main-sequence phases. The evolutionary sequences for LY, SC and OV_1 nearly coincide in most evolved models, M3e, because in these models the signature of mixing processes has been nearly erased. The OV_2 is still far away because the chemically inhomogeneous zone extends well above the source.

Applications of the $\bar{d} - d_S$ diagrams is limited to the cases where the modes partially trapped do not appear in the frequency domain of solar-like oscillations. Signature of such partial trapping are rapid changes of the small separations, such as seen in Figure 6. The rapid changes are in fact a very sensitive probe of mixing processes, but make our two parameters, \bar{d} and d_S , not well defined. Our calculations for $1.3 M_\odot$ indicate that the post main-sequence phase, where we may trust in \bar{d} and d_S , lasts about 0.6 Gyr for weak mixing scenarios.

5. Summary

We have analyzed the small separations of a representative set of evolutionary models of moderate ($1.2 - 1.9 M_\odot$) mass stars with different scenarios of mixing beyond the convective core. Four mixing scenarios were taken into account, layered scenario (LY), semiconvective scenario (SC) and two overshooting scenarios of different extent (OV_1 , OV_2). Our numerical results for two types of small separations, d_{01} and d_{02} , indicate that within the frequency range of p-modes, d_{01} is more sensitive to mixing scenarios than d_{02} . Our simple parametrization of d_{01} by the mean value, \bar{d} , and the slope, d_S , enables us to compare models and observations on a single $\bar{d} - d_S$ diagram.

We have found that the location of a star on the diagram depends on its evolutionary status and the mixing scenario. During the main-sequence phase stars evolve slowly toward higher slopes, d_S . During this phase, stars having different mixing scenarios may be distinguished with \bar{d} , which is correlated with the extent of mixing. The higher is the extent of mixing, the larger is \bar{d} . This correlation allows to determine the extent of mixing with an accuracy depending on the accuracy of frequency measurements. For example, $0.2H_p$ difference in the mixing extent manifests as a difference of approximately $0.7\mu\text{Hz}$ in \bar{d} . Such an accuracy of \bar{d}

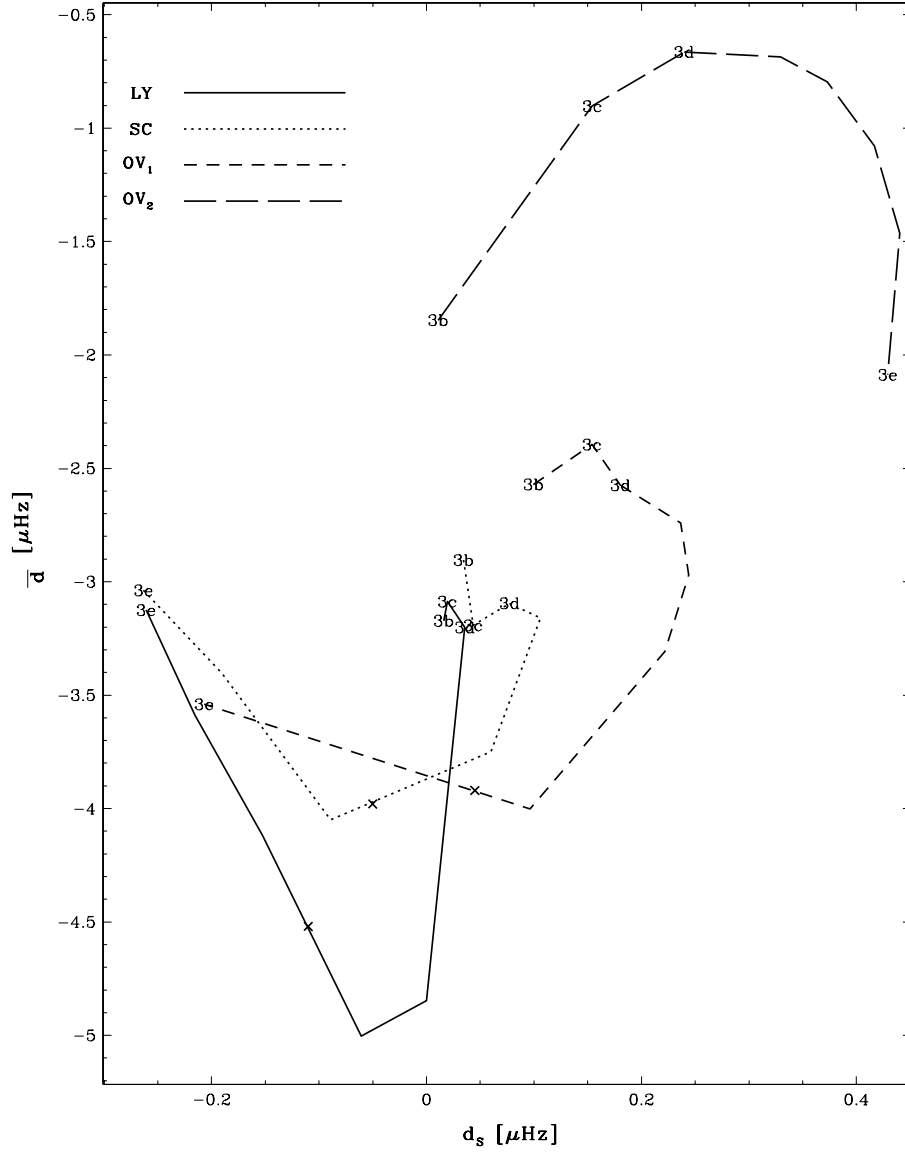


Figure 10: Diagnostic diagram for $1.3 M_{\odot}$. The same as in Figure 9 but including the most evolved models of our survey, ie M3e. Cross indicates the TAMS model on each track extending to the post main-sequence phase, ie LY, SC and OV_1 tracks. All M3e models, which are post main-sequence stars, are located in the domain of low slopes.

requires the frequency accuracy of $1.8\mu\text{Hz}$ or better. Optimistic predictions of the frequency accuracy for space missions give a much better value of $0.1\mu\text{Hz}$. The discrimination between two scenarios of low mixing extent, SC and LY, is difficult for young main-sequence objects because their values of (\bar{d}, d_S) overlap. We show, however, that the distinction is possible for the most evolved main-sequence stars. Similar SC and LY stars in this phase may differ as much as $1\mu\text{Hz}$ in \bar{d} , what requires the frequency accuracy of $2.6\mu\text{Hz}$ or better. Such stars are characterized by a rapid evolution of their cores. During this phase such star moves rapidly towards low slopes on the $\bar{d} - d_S$ diagram. Identification of the mixing scenario is still possible for such star but requires strong constraints on other stellar observables like effective temperature, radius, metallicity and age.

Acknowledgements. This work was supported in part by the Polish State Committee for Scientific Research grant 2-P03D-14.

REFERENCES

- Alexander, D.R., and Ferguson, J.W. 1994, *Astrophys. J.*, **437**, 879.
- Baglin, A., Auvergne, M., Barge, P., Buey, J.T., Catala, C., Michel, E., Weiss, W., and the COROT Team 2002, *Proc. of 1st Eddington workshop "Stellar Structure and Habitable Planet Finding"*, 17, <http://corot.asrsp-mrs.fr/>.
- Biello, J.A. 2001, astro-ph/0102338.
- Christensen-Dalsgaard, J., and Frandsen, S. 1988, (eds.) *Advances in Helio- and Asteroseismology, IAU Symp. (D.Reidel Publ. Co., Dordrecht)*, **123**, 295.
- Crowe, R.A., and Mitalas, R. 1982, *Astron. Astrophys.*, **108**, 55.
- Dziembowski, W.A. 1977, *Acta Astron.*, **27**, 95.
- Grevesse, N., and Noels, A. 1993, *Phys. Scr.*, **T47**, 133.
- Houdek, G., Balmforth, N.J., Christensen-Dalsgaard, J., and Gough, D.O. 1999, *Astron. Astrophys.*, **351**, 582.
- Iglesias, C.A., and Rogers, F.J. 1996, *Astrophys. J.*, **464**, 943.
- Kato, S. 1966, *Publ. Astron. Soc. Japan*, **18**, 374.
- Ledoux, P. 1947, *Astrophys. J.*, **105**, 305.
- Martić, M., Lebrun, J.-C., Appourchaux, T., and Korzennik, S.G. 2004, *Astron. Astrophys.*, **418**, 295.
- Rogers, F.J. 2001, *Contributions to Plasma Physics*, **41**, 179.
- Roxburgh, I.W. 1993, *PRISMA, Report of Phase a Study*, eds. T.Appourchaux et al. , *ESA SCI(93)*, 31.
- Roxburgh, I.W. and Favata, F. 2003, *Astrophysics and Space Science*, **284**, 17.
- Roxburgh, I.W. and Vorontsov, S.V. 1994, *Mon. Not. R. astr. Soc.*, **267**, 297.
- Schwarzschild M. 1906, *Gott. Nach.*, **1**, 41.
- Schwarzschild M. and Härm, R 1958, *Astrophys. J.*, **128**, 348.
- Shaller, G., Shaerer, D., Meynet, G., and Maeder, A. 1992, *Astron. Astrophys. Suppl. Ser.*, **96**, 269.
- Spruit, H.C. 1992, *Astron. Astrophys.*, **253**, 131.
- Stevenson, D.J. 1979, *Mon. Not. R. astr. Soc.*, **187**, 129.
- Tassoul, M. 1990, *Astrophys. J.*, **358**, 313.
- VandenBerg, D.A. 1985, *Astron. Astrophys. Suppl. Ser.*, **58**, 711.
- Walker, G., Matthews, J., Kuschnig, R., Johnson, R., Rucinski, S., Pazder, J., Burley, G., Walker, A., Skaret, K., Zee, R., Grocott, S., Carroll, K., Sinclair, P., Sturgeon, D., and Harron, J. 2003, *PASP*, **115**, 1023.